J. Fluid Mech. (1972), *vol.* 56, *part* 1, *pp.* 173–192
Printed in Great Britain

Solution of the wedge entry problem by numerical conformal mapping

By O. F. HUGHES

School of Mechanical and Industrial Engineering,
The University of New South Wales

(Received 3 February 1972)

An accurate quasi-analytic method of solution is presented for the classical hydrodynamics problem of the constant-velocity entry of a prismatic wedge into a weightless incompressible inviscid fluid. The method uses the Wagner function W, which reduces the problem to the determination of a mapping function $\Lambda = \mathscr{L}(W)$ for the hodograph. $\mathscr{L}(W)$ is constructed by using the hodograph for an unsymmetric diamond together with a modifying or 'preparatory' transformation. A computer method of conformal mapping is developed and is used to obtain this latter transformation. Results are presented for the case of a 90° wedge and show that the solution is both more accurate than previous solutions, having an error of less than 1 %, and more complete, as it portrays the entire flow field and furnishes information about the functional dependence among the variables.

1. Introduction

A problem which poses great difficulty in fluid mechanics is that of determining the pressure distribution on a solid structure due to impact with the free surface of a fluid. The most common example is the classical problem in which a prismatic wedge-shaped body penetrates the free surface of an ideal incompressible fluid at constant speed. First posed by Wagner (1932) in relation to the landing of seaplanes, this idealized problem may also be applied to the 'bow flare' impact of ships in heavy seas, the performance of planing craft and other cases of free-surface penetration involving large fluid accelerations. The principal difficulty involved is that of satisfying the nonlinear constant-pressure condition on the free surface, whose location is unknown and must be found as part of the solution. Previous methods of solution may generally be grouped into two categories.

(i) Solutions which specify the flow analytically (generally by an equivalent body approach) but only very approximately. Examples are those of Shiffman & Spencer (1951), Bisplinghoff & Doherty (1952) and Fabula (1957).

(ii) Numerical solutions to the complete boundary-value problem formulated by Wagner, of which the most significant are those of Garabedian (1953, 1965), Borg (1957) and Dobrovolskaya (1963, 1964, 1969).

Although the latter are more accurate, being numerical solutions they do not shed much light on the qualitative aspects of the problem such as the presence or

absence of singularities anywhere in the flow field, the location and type of these singularities and the functional dependence of the variables. In a word, these numerical solutions do not give a 'picture' of the flow. This is in direct contrast to the first group of solutions, in which an analytically specified flow is used as a model to approximate the unknown flow, but with a concomitant loss of accuracy due to this approximation. The present work goes beyond these previous analyses and combines their best features by presenting a solution which is both analytic and accurate.

2. Problem formulation

To simplify the subsequent analysis, we consider the equivalent case in which the wedge is stationary and the fluid moves towards it at constant speed C. Because of symmetry only one side of the wedge need be considered, and in figure 1 the wedge centre-line is placed along the X axis so that the fluid region lies in the first quadrant of the X, Y plane. The flow is therefore from right to left and the fluid velocity at infinity is $-C$. The fluid is assumed to be incompressible, inviscid and initially undisturbed. The latter two assumptions cause the flow to be irrotational. One further simplification which is essential to the classical wedge penetration problem solved here is that the effect of gravity is ignored. As was shown by Wagner, this assumption causes the flow to be geometrically self-similar, for which the velocity potential $\phi(X, Y, t)$ satisfies the homogeneity relation

$$\phi(X, Y, t) = C^2 t \phi(x, y), \tag{2.1}$$

where

$$x = X/Ct, \quad y = Y/Ct. \tag{2.2}$$

The dimensionless variables x and y of (2.2) reduce the above unsteady flow to a steady-state boundary-value problem for the transformed potential $\phi(x, y)$. In the x, y plane of figure 2 the free-surface height $h = H/Ct$ and the fluid velocities $u = U/C$ and $v = V/C$ are all dimensionless. The free-surface curve $h(y)$ is now fixed in position and the wedge depth is unity.

The various boundary conditions of the problem have been derived fully by Wagner and subsequent authors for both the physical (X, Y) plane and the transformed (x, y) plane. For the latter case, they are as follows.

(a) Constant pressure on the free surface:

$$p/\rho C^2 = -\phi + xu + yv - \tfrac{1}{2}(u^2 + v^2 - 1) = 0. \tag{2.3}$$

(b) Zero velocity normal to the wedge:

$$\partial\phi/\partial n = 0.$$

(c) Symmetry: $\partial\phi/\partial y = 0$ along x axis.

(d) Decay of disturbance velocity at large distances:

$$\partial\phi/\partial x \to -1, \quad \partial\phi/\partial y \to 0 \quad \text{as} \quad x^2 + y^2 \to \infty.$$

(e) Conservation of mass, which requires that the volume (or area, for two-dimensional flow) of fluid displaced above the original free surface must equal the immersed volume (or area) of the wedge below the original free surface.

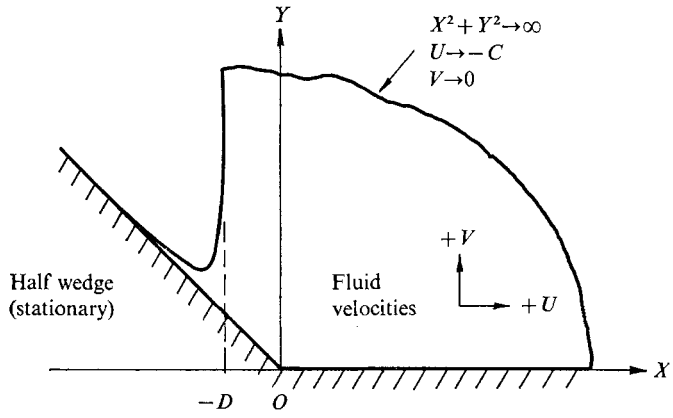

FIGURE 1. Co-ordinate system: physical plane.

(*f*) Also, there is a kinematic condition, stemming from the fact that for irrotational flow the free surface always consists of the same particles. Thus the rate of change of the free-surface height is equal to the upwards velocity of fluid particles on the free surface. If, as in figure 2, $\tan\theta = dy/dx$ denotes the slope of the free surface, it may be demonstrated that the above condition is expressed by

$$\tan\theta = (y-v)/(x-u). \tag{2.4}$$

In order to use the methods of complex analysis we define $z = x+iy$ as the complex flow plane and $w = u+iv$ as the complex velocity. In figure 2 the z plane and the w plane are superimposed. Among other things, this figure illustrates the fact, which is due to the geometric similarity, that at the spray tip the magnitude of the velocity is numerically equal to the distance from the nose of the wedge, i.e. $w_t = z_t$.

Of the many observations and contributions to the problem made by Wagner, probably the most valuable is the geometric relationship which he derived from the constant-pressure condition. This was presented in a footnote of his paper and its significance seems not to have been realized until Man (1957), in a thesis supervized by Sedov, corrected an error which Wagner had made and proved the relationship conclusively.

Wagner's observation is based on the well-known fact that a free surface is always aligned perpendicularly to the local direction of acceleration. As is shown in figure 2, a change in velocity dw is incurred when moving through a distance dz along the free surface. This change in velocity implies an acceleration and thus the differential element dw must be perpendicular to dz. If, in place of w, we introduce its negative conjugate $\Lambda = -\overline{w}$, then the above statement implies that the product $d\Lambda\, dz$ will always be negative imaginary, having an argument $-\frac{1}{2}\pi$. We therefore define

$$dW = (d\Lambda\, dz)^{\frac{1}{2}}, \tag{2.5}$$

and the condition of constant pressure is then equivalent to requiring $\arg(dW) = -\frac{1}{4}\pi$ at every point along the free surface. Thus, the integration of

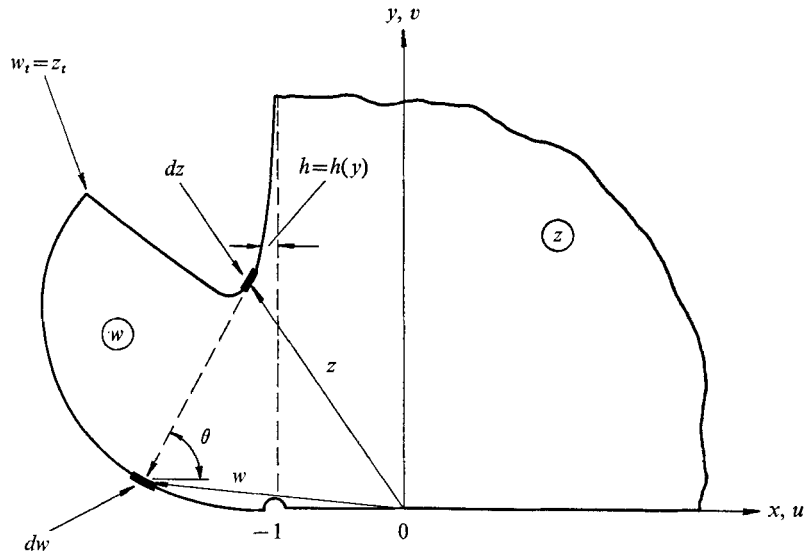

FIGURE 2. Vector diagram of complex quantities.

dW along the free surface, starting at the spray tip, results in a straight line whose argument is $-\frac{1}{4}\pi$, namely:

$$W(z) = \int_{z_t}^{z} (d\Lambda\, dz)^{\frac{1}{2}}. \tag{2.6}$$

This function will be referred to as the Wagner function. As a mapping function, $W(z)$ is extremely useful since it transforms the unknown curve of the free surface in the z plane into a straight line in the W plane. The other boundaries of the fluid region are straight lines, both in the z plane and in the Λ plane. They will therefore continue to be straight lines when transformed into the W plane. In his dissertation Man proved that all three boundary lines are of finite length in this plane. Thus, the Wagner function maps the entire fluid region of the z plane into an isosceles (45°) right triangle. The W plane is shown in the upper left-hand corner of figure 4 and the fluid region is the triangle in the lower left-hand portion of the plane. The Wagner function was first applied successfully to the wedge problem by Dobrovolskaya (1963); she has also pointed out (Dobrovolskaya 1969) the generality of its application to free-surface problems.

3. Conformal-mapping method of solution

Since the shape of the fluid region is known in the W plane, the plane defined by the Wagner function, the ensuing analysis will use W as the independent variable and all other quantities will be expressed in terms of W. Also, instead of attempting to solve for the complex potential we shall solve for its derivative, which corresponds to the velocity. Specifically, we shall solve for $\Lambda(W)$, where Λ is the negative conjugate of the velocity, and its related to the complex potential Ω by

$$\Lambda = -d\Omega/dz.$$

Let us denote this unknown function by

$$\Lambda = \mathscr{L}(W). \tag{3.1}$$

In terms of conformal transformation $\mathscr{L}(W)$ is a mapping function which transforms the triangular fluid region of the Wagner plane into the hodograph Λ.

The definition of dW in (2.5) can be rearranged to give

$$dW/dz = \mathscr{L}'(W), \tag{3.2}$$

in which the prime denotes differentiation with respect to W. From this it follows that

$$z = \int \frac{dW}{\mathscr{L}'(W)}, \tag{3.3}$$

and since $\Lambda = -d\Omega/dz$ it is also possible to obtain an integral expression for Ω:

$$\Omega = -\int \frac{\mathscr{L}(W)}{\mathscr{L}'(W)} dW. \tag{3.4}$$

The unknown function $\mathscr{L}(W)$ is thus capable of providing a complete solution to the problem and the next few sections are directed toward the determination of this function. The use of (3.1), (3.3) and (3.4) as mapping functions is illustrated in figure 4 below, which shows the $W \rightarrow \Lambda$ transformation as a sequence of three successive mappings. The ζ plane in figure 4 is a plane of uniform flow from right to left and ζ is thus directly related to the complex potential: $\Omega = -\zeta$. In terms of ζ, the hodograph variable Λ becomes $\Lambda = d\zeta/dz$.

4. Method for obtaining velocity

It is a well-established fact that a body penetrating a free surface is always a 'finite' body, regardless of its shape or size outside the fluid, since only its wetted portion causes disturbance in the fluid. Thus, at large $|z|$ the flow pattern for the wedge may be replaced by that of some equivalent body fully submerged in a uniform stream. The majority of the previous treatments of the wedge problem have used the equivalent body approach but with several simplifying approximations.

(i) The equivalent body is assumed to have a transverse axis of symmetry parallel to the y axis. For a wedge this gives a symmetric diamond-shaped body, having zero transverse velocity v along this axis of symmetry and infinite velocity at the lateral corner points.

(ii) The free-surface velocity is taken to be that along this transverse axis of symmetry; that is, the transverse or v component of the velocity is assumed to be zero on the free surface.

(iii) The diamond-shaped equivalent body is used as a direct replacement for the wedge, thus causing the point of infinite velocity to lie on the face of the wedge.

In order to obtain some information about the true velocity distribution, the first step in the present investigation was to obtain a numerical solution of the case of a 90° wedge, using the relaxation method of Borg (1957). From the results (which are not presented here for the sake of brevity) it was evident that over

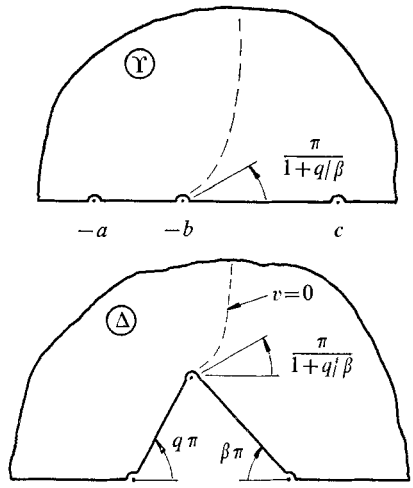

FIGURE 3. Hodograph transformation for an asymmetric diamond.

most of the flow plane the diamond-shaped equivalent body gives an accurate representation of the flow. Furthermore, it appeared that the velocity distribution in the spray-root region could be accurately represented by a point of infinite velocity, located at the approximate centre of curvature of the free surface (point B in the z plane of figure 4). That is, the actual wedge flow seemed to possess a singularity similar to that of the diamond-shaped equivalent body, but not on the wedge itself, nor in the fluid, but *outside* the fluid region. Thus the diamond-shaped equivalent body appeared to be a suitable starting-point for a conformal-mapping type of solution. However, instead of being used as a direct replacement for the wedge, it is here used as a basic model for the hodograph Λ.

Moreover, the incorrect assumption of zero transverse velocity on the free surface can easily be avoided by simply dropping the requirement that the diamond should have a transverse axis of symmetry. We thus have the more general case of an asymmetric diamond, such as that shown in figure 3. The mapping function which will produce this shape is given in derivative form by the Schwarz–Christoffel formula as

$$\frac{d\Upsilon}{d\Delta} = \Lambda_D(\Upsilon) = \frac{(\Upsilon+a)^q(\Upsilon-c)^\beta}{(\Upsilon+b)^{q+\beta}}. \tag{4.1}$$

The meaning of each parameter is evident from figure 3. It may be shown that the corner angles and lengths of sides are related by

$$q(a-b) = \beta(b+c). \tag{4.2}$$

If the Υ plane is interpreted as a plane of uniform flow, (4.1) represents the velocity Λ_D corresponding to the flow about an asymmetric diamond in the Δ plane. As can be seen in figure 3, the shape of the $v = 0$ line is now more general and is a straight line only for the case of a symmetric diamond ($q = \beta$). Thus, provided that the trailing angle $q\pi$ is correctly chosen, the true wedge velocity Λ could be accurately represented over most of the flow plane by applying the

mapping function Λ_D to the ζ plane, the plane of uniform flow. However, in the spray-root region the wedge flow differs from that of an asymmetric diamond, at least in regard to the location of the point of infinite velocity. Thus, if Λ_D is used to obtain Λ, the plane on which it operates cannot be the ζ plane but must instead be some other plane, say the Υ plane, such that when (4.1) is applied to Υ it produces the correct hodograph Λ for the *entire* flow field. In other words, the variable Υ in (4.1) is now given a special role: it must be such as to provide whatever modifications are required regarding the nature and location of the spray-root singularity. Since we wish to obtain Λ in the form $\Lambda = \mathscr{L}(W)$ it will be necessary to obtain Υ as a function of W. In effect, the unknown mapping function $\mathscr{L}(W)$ is being subdivided into two functions, $\Upsilon(W)$ and $\Lambda(\Upsilon)$, and the first of these becomes the new unknown in the problem.

Following this approach, even an approximate solution for $\Upsilon(W)$ quickly reveals that the shape of the fluid region in the Υ plane is very nearly a quarter plane. The triangular shape of the W plane can easily be converted to a quarter plane by the elliptic function transformation $\Gamma = T_e(W)$ given below in equation (7.1). The resulting similarity between Γ and Υ is of great assistance, since it minimizes the changes required of the unknown mapping function. Hence, this further subdivision is adopted here and the transformation from Γ to Υ is now the unknown or 'missing link' in the chain of transformations which constitute $\mathscr{L}(W)$. Since it is employed near the beginning of the solution process and since its purpose is to convert the Γ plane into one which is suitable for the hodograph transformation, it will be referred to as the 'preparatory transformation'. For convenience, the symbol T_p will be used to indicate this transformation: $\Upsilon = T_p(\Gamma)$.

5. Basic properties and parameters

As a first step in the solution, we examine the mapping parameters which specify the nature and location of the singularities. The points which are known or suspected to be singularities are the following.

Spray-tip singularity ($\Gamma = 0$)

Let us denote the angle in the z plane at which the fluid surface meets the wedge as τ. This quantity has been the subject of much discussion in the literature. Early workers, such as Wagner, intuitively assumed this to be a small but finite angle, and the numerical solutions of Pierson (1950) and Borg (1957) clearly show that to be the case. However, the later and more theoretical analyses differed widely in their conclusions, some maintaining that $\tau = 0$ and others that $\tau = \frac{1}{2}\pi$. This long-standing disagreement was resolved by Hughes (1971), who showed that τ is small but finite, that the spray-tip angle in the ζ plane is also equal to τ and that the corresponding angle in the Λ plane is $\frac{1}{2}\pi - \tau$. In the same work it is also shown that at the spray tip the functional relationship between Λ and Γ is

$$\Lambda - \Lambda_t = C_1 \Gamma^{1-\alpha}, \tag{5.1}$$

in which C_1 is an unspecified complex constant and α is a non-dimensional parameter related to τ by

$$\tau = \tfrac{1}{2}\alpha\pi. \tag{5.2}$$

This in turn requires that in the transformation from Γ to Λ the right angle at $\Gamma = 0$ be reduced to $\frac{1}{2}(1-\alpha)\pi$ in the Λ plane. Since this change of angle cannot be obtained from $\Lambda_D(\Upsilon)$ it must be supplied by the preparatory transformation $\Upsilon = T_p(\Gamma)$. Thus, one of the basic features which the latter must have is that near the spray tip Υ must be proportional to $\Gamma^{1-\alpha}$. That is,

$$\Upsilon(\Gamma) \propto \Gamma^{1-\alpha} \quad \text{at} \quad \Gamma = 0. \tag{5.3}$$

Spray-root singularity ($\Gamma = \Gamma_b$)

The part of the flow plane which is of greatest interest is the area in the vicinity of the spray root, the point where the slope of the free surface becomes vertical, since it is here that the curvature of the free surface (and therefore the velocity, pressure, etc.) is changing most rapidly. As was mentioned earlier, an initial relaxation solution seemed to indicate the existence of a point of infinite velocity in the approximate centre of curvature of the free surface. Since the solution was merely numerical and since the suspected singularity was situated outside the fluid region, it was not possible to determine its precise nature and location by this method. Nevertheless, the possibility of such a point was clearly indicated, giving rise to the hypothesis that in this region the velocity (and hence the hodograph variable Λ) is proportional to some inverse power of the distance from the suspected singularity point. If we denote the location of this point in the Γ plane as Γ_b and if χ denotes the inverse power, then the relationship is

$$\Lambda(\Gamma) \propto 1/(\Gamma - \Gamma_b)^{\chi} \quad \text{at} \quad \Gamma = \Gamma_b. \tag{5.4}$$

In the Υ plane of figure 4 this point is $\Upsilon = -b$ and it is clear from (4.1) that at this point there is an algebraic singularity of order $q+\beta$. However, the $\Gamma \to \Lambda$ transformation is being performed in two stages and to be completely general we must also allow for a singularity to occur at the corresponding point in the first or preparatory transformation $T_p(\Gamma)$. The singularity of order χ in the overall $\Gamma \to \Lambda$ transformation is then the resultant of these two. If η denotes the order of the (possible) singularity in the preparatory transformation then

$$\chi = \eta(q+\beta). \tag{5.5}$$

Other singularities

The other two points in the Γ plane which are known to be singularities are $\Gamma = \pm\epsilon$. The point $\Gamma = \epsilon$ corresponds to the nose and for a straight-sided wedge the relationship between Γ and Λ at this point must be

$$\Lambda(\Gamma) \propto (\Gamma - \epsilon)^{\beta}. \tag{5.6}$$

This relationship is exactly satisfied by the diamond mapping function of (4.1), in which c is the point in the Υ plane corresponding to $\Gamma = \epsilon$. Therefore, this point should *not* be a singularity in the preparatory transformation. On the other hand, the point $\Gamma = -\epsilon$ does not have any predetermined role in the $\Gamma \to \Lambda$ transformation and nothing can be concluded about it at this stage.

6. A computer-oriented method of conformal transformation

As formulated above, the problem consists essentially in determining the preparatory transformation $\Upsilon = T_p(\Gamma)$. In general, the task of finding a mapping function is a trial-and-error process. Although a few direct techniques have been developed for specific cases (such as the Schwarz–Christoffel theorem), it may be said that in most cases solutions are found either by laboriously trying various combinations of known mapping functions or by solving the inverse problem (i.e. specifying a mapping function and searching for an application). For the problem at hand, a method is required which easily incorporates both known and suspected singularities, the latter being expressed in terms of parameters whose values can then be found from the conditions of the problem. In order to meet this need, a computer-oriented method of conformal mapping was developed, based on the generalized circle transformation $P = T_c(\Pi)$. This transformation can best be represented by a sequence of two transformations:†

$$\Xi = \left(\frac{\Pi-\lambda}{\Pi-\kappa}\right)^{\mu}, \quad P = \frac{\mu(\lambda-\kappa)}{2}\frac{1+\Xi}{1-\Xi}+\frac{\lambda+\kappa}{2}.$$

In essence, the method consists of using the generalized circle transformation repeatedly, in different parts of the flow plane, in order to produce the required overall transformation. Each application operates on the result of the previous one and each is aimed at producing a particular aspect of the desired overall transformation. The generalized circle transformation is well suited for this type of application, as may be seen from the following considerations.

(i) It is general, because variations in its parameters can produce changes in location (determined by the sum of κ and λ), size (determined by the difference of κ and λ) and shape (determined by the value of μ, ranging from 0 to ∞, with $\mu = 1$ corresponding to a null transformation).

(ii) It is simple, in that it contains only three parameters and these are directly related to the singularity points. Also, it is symmetric about the real axis.

(iii) It is localized in its effect; as $|\Pi| \to \infty$, $T_c(\Pi) \to \Pi$.

Another advantage of using a single basic mapping function is the fact that the derivative can be calculated easily and analytically, thereby obviating the need for time-consuming (and often inaccurate) numerical differentiation, this is of great importance in the wedge problem since the physical or z plane is to be obtained by means of the derivative $d\Lambda/dW$ in (3.3).

7. Summary of transformations and associated parameters

The preparatory transformation, which is the principal 'unknown' in the problem, was obtained by means of the above method. Four applications of the basic mapping function $T_c(\Pi)$ were required. Each has three parameters, and another parameter Q was used in the third mapping, giving a total of thirteen. However, seven of the parameter values were specified by problem requirements

† An alternative formation using 'coaxial co-ordinates' is given in §6.51 of Milne-Thomson (1938).

or were predetermined from earlier values, leaving six undetermined parameters: $\mu_1, \mu_2, \kappa_2, Q, \mu_3$ and μ_4. Details of the mapping are given in the appendix.

The other transformations are the mapping from the W to the Γ plane, which transforms the triangular region of W into a quarter plane, and the hodograph mapping from the Υ to the Δ plane which follows the preparatory transformation. The first transformation, denoted symbolically as $\Gamma = T_\epsilon(W)$, is an elementary elliptic function transformation:

$$\Gamma = T_\epsilon(W) = \frac{\epsilon}{2}\left[\frac{\mathrm{sn}\,(iW/m)}{\mathrm{dn}\,(iW/m)}\right]^2. \tag{7.1}$$

The period of this expression in both the real and imaginary directions of W is equal to mK, where K is the value of the complete elliptic integral of order 0·707, which from the handbooks is 1·8541. The parameter m is a measure of the size of the triangle in the W plane and the parameter ϵ specifies the location of the two points in the Γ plane corresponding to the 45° corners of the Wagner function triangle. Both m and ϵ are undetermined parameters and must be included as such in the solution.

The final transformation is the hodograph mapping from the Υ to the Λ plane, which uses the asymmetric diamond mapping function of (4.1). The only aspect requiring further discussion is the role played by the four parameters of this transformation. Three of its four parameters are singularity points ($-a$, $-b$ and c) and the latter two can be calculated from points defined in preceding planes (κ_4 in the Π_3 plane and ϵ in the Γ plane, respectively). However, the parameter a is unknown and must be added to the list of undetermined parameters. The fourth parameter, the exponent q, can be determined from (4.2).

At this stage we have introduced a total of nine undetermined parameters into the problem: six from the preparatory transformation, one from $\Lambda_D(\Upsilon)$ and two others from the $W \to \Gamma$ transformation. Some of these parameters are exponents and in several cases these are applied at the two most significant singularity points: the spray root and the spray tip. Therefore, these exponents are directly related to the order of the overall singularity at these points. For the spray tip it can be shown from (5.3) that $\alpha = 1 - \mu_1\mu_3\mu_4$ and for the spray-root singularity the corresponding relation is $\eta = \mu_2\mu_4$, since η denotes the order of this singularity in the preparatory transformation.

8. Other parameters and problem conditions

Two of the conditions, the requirement of zero pressure and the kinematic condition, must be satisfied along the entire free-surface boundary. The location of this curve can be determined by substituting $\mathscr{L}'(W)$ into (3.3) and integrating but the expressions for $\mathscr{L}(W)$ and $\mathscr{L}'(W)$ obtained from the conformal mapping will generally be far too complicated for analytical integration and numerical integration must be used. This in turn means that the position of the free surface cannot be obtained as an equation; instead, the calculation must consist of a point-by-point numerical integration of (3.3). The location and velocity of each point can then be inserted into (2.3) and (2.4) to test whether the two surface

conditions are fulfilled. In order to avoid having to satisfy two conditions at each point, the kinematic condition can be satisfied implicitly by being used to calculate the slope of the free surface at each point. In this approach the independent variable is the arc length s along the free surface and (2.4) and (3.3) constitute two simultaneous differential equations. These may be rewritten as

$$dz/ds = \exp\{i \arg[z + \overline{\mathscr{L}(W)}]\} \tag{8.1}$$

and

$$dW/dz = \mathscr{L}'(W). \tag{8.2}$$

Hughes (1971) has shown that for reasons of stability the numerical integration of (8.1) must be done in an inwards direction, starting at some point z at a large distance from the wedge. He also showed that expressions can be derived for the various free-surface quantities which give the starting values for this integration. However, the corresponding starting-point in the W plane is unknown and must therefore be treated as an undetermined parameter, $|W_0|$, bringing the total number of such parameters to ten. (Since the argument of W_0 is $-\frac{1}{4}\pi$, only the magnitude is unknown.)

Beginning with these initial values, the differential equations (8.1) and (8.2) can be solved by any of the standard techniques. The integration is continued until $s = 0$, which corresponds to the spray tip. At this point the value of W should be zero and this constitutes an additional condition which must be satisfied. One further condition which must be satisfied is that the nose of the wedge must correspond to $W = -imK$. This can be examined by integrating (8.2) from the spray tip to the nose. If W_n denotes the final value of W obtained by this process, then the error is $e = |W_n + imK|$.

9. Solution for parameter values; accuracy of results

In general terms, the method of solution consists of solving the problem by means of $\mathscr{L}(W)$ using initial (or current) estimates for all of the parameter values and thus determining the degree to which these values satisfy the various conditions of the problem. The degree of accuracy is measured by error terms, each of which corresponds to one of the conditions. Since there are ten parameters, there must be ten such conditions. Of the six basic conditions listed in § 2, three have been satisfied automatically in the formulation of $\mathscr{L}(W)$ (normal velocity, symmetry and velocity decay) and therefore cannot be used for the determination of parameters. Also, the kinematic condition has been implicitly satisfied in determining the free-surface location. On the other hand, two further conditions relating to the W plane were introduced above ($W_t = 0$ and $W_n = -imK$). This gives a total of four conditions and seems to leave a deficiency of six. However, one of these four is the pressure condition which must be satisfied along the entire free surface, and all of the numerous values of pressure calculated during the free-surface integration can be used as measures of error. In the present case, seven of these pressure values must be selected in order to make up the required total of ten error terms. The result is a system of ten simultaneous nonlinear equations which may be solved by an iterative numerical technique such as the generalized Newton–Raphson method.

Parameter	Preliminary solution	Modified solution	Error term, e_i	Preliminary solution	Modified solution
μ_1	0·496	0·5*	$e_1 = \lvert W_t \rvert$	0·00025	−0·00050
μ_2	0·834	0·834	$e_2 = A - A_0 - \frac{1}{2}$	0·00107	0·00125
κ_2	0·322	0·321	$e_3 = W_n + imK$	−0·00156	0·00102
Q	0·672	0·671	$e_4 = p/\rho C^2$ at $s = 4·0$	−0·00003	0·00001
μ_3	2·034	2·0*	$e_5 = p/\rho C^2$ at $s = 2·0$	−0·00027	0·00015
μ_4	0·958	0·960	$e_6 = p/\rho C^2$ at $s = 1·75$	0·00008	0·00032
a	1·252	1·254	$e_7 = p/\rho C^2$ at $s = 1·5$	0·00462	0·00554
m	1·450	1·450	$e_8 = p/\rho C^2$ at $s = 1·25$	0·00060	0·00034
ϵ	1·032	1·928	$e_9 = p/\rho C^2$ at $s = 1·0$	0·00017	0·00004
$\lvert W_0 \rvert$	2·585	2·582	$e_{10} = p/\rho C^2$ at $s = 0$	$3·0 \times 10^{-7}$	$-1·0 \times 10^{-7}$
α	0·040	0·040	—	—	—
q	1·012	1·0*	—	—	—
χ	1·010	1·0*	—	—	—

TABLE 1. Parameter values and solution errors.
An asterisk denotes a fixed value.

The resulting parameter values and error terms for a 90° wedge are given in table 1 under the heading 'Preliminary solution'. This heading emphasizes the fact that the individual transformations may have some small and extraneous quirks as a result of the solution process. An obvious instance is the case in which parameter values are very close to being exact geometrically simplifying values. The test as to whether a slight disparity or other small complication should be eliminated is the error (in boundary conditions, etc.) which is thus introduced. If it is negligible, then the disparity is probably extraneous to the solution and the simplification should be made. Therefore the parameter values given in table 1 were examined to determine what overall transformation is being implied and to check for any obvious simplifications. There are four such cases and the simplified parameter values are indicated by asterisks in the column headed 'Modified solution', together with the corresponding values obtained for the other parameters when these four were given their prescribed values. A comparison of error terms shows that there is no significant increase in error; a slight increase has occurred in some cases and in other cases the error has diminished. This confirms the advisability of making these simplifications. It should be noted that all the error terms in table 1 are for non-dimensional quantities which are either equal to, or of the order of, unity. Therefore, these error terms may be considered as relative errors, as well as absolute. Moreover, they are a direct indication of the accuracy of the solution, which in problems of this type is measured by the extent to which the boundary conditions are fulfilled. The accuracy of the solution is considered to be excellent, since at no point does the error exceed 1 % and in most cases it is well below this figure.

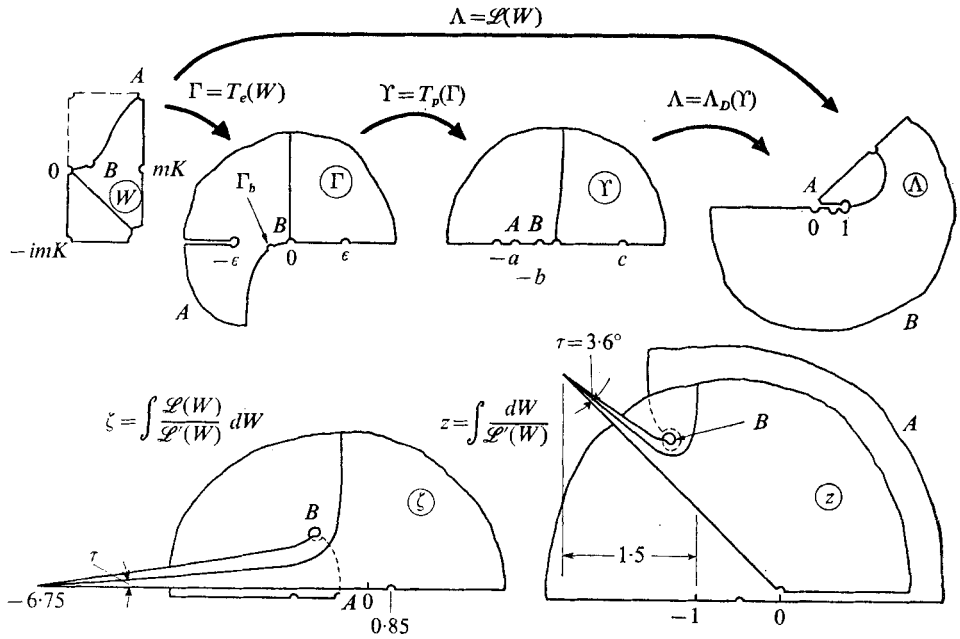

FIGURE 4. Overall transformation for Λ, ζ and Z.

10. Discussion of results

The various transformations corresponding to the modified parameter values are shown in figures 4 and 5. Most of the features of the solution can be discerned from these figures and only the more salient points will be discussed.

Spray-root singularity

Possibly the most interesting feature of the flow is the singularity which has been shown to occur in the spray-root region. The present analysis appears to be the first to have specifically postulated such a feature and the accuracy of the resulting solution is doubly gratifying inasmuch as the entire method was based on this postulate. With regard to the order of this singularity, the solution given in table 1 shows that $\chi = 1{\cdot}0$, and thus in the Γ plane the singularity is a simple pole. From this it can be shown, using (3.3) and (3.4), that

$$(z - z_b) = C_2(\zeta - \zeta_b)^{\frac{3}{2}}, \tag{10.1}$$

which indicates the precise nature of the spray-root singularity in the transformation from the ζ to the z plane (C_2 is an arbitrary complex constant).

Wedge pressure distribution

Figure 6 shows a plot of the non-dimensional pressure $p/(\frac{1}{2}\rho C^2)$ along the face of the wedge. The secondary pressure peak near the spray root is a well-known feature of the wedge problem; for wedge angles greater than about 100° this pressure exceeds the stagnation pressure at the nose of the wedge. Inasmuch as the measure of error in problems of this type is the extent to which the boundary

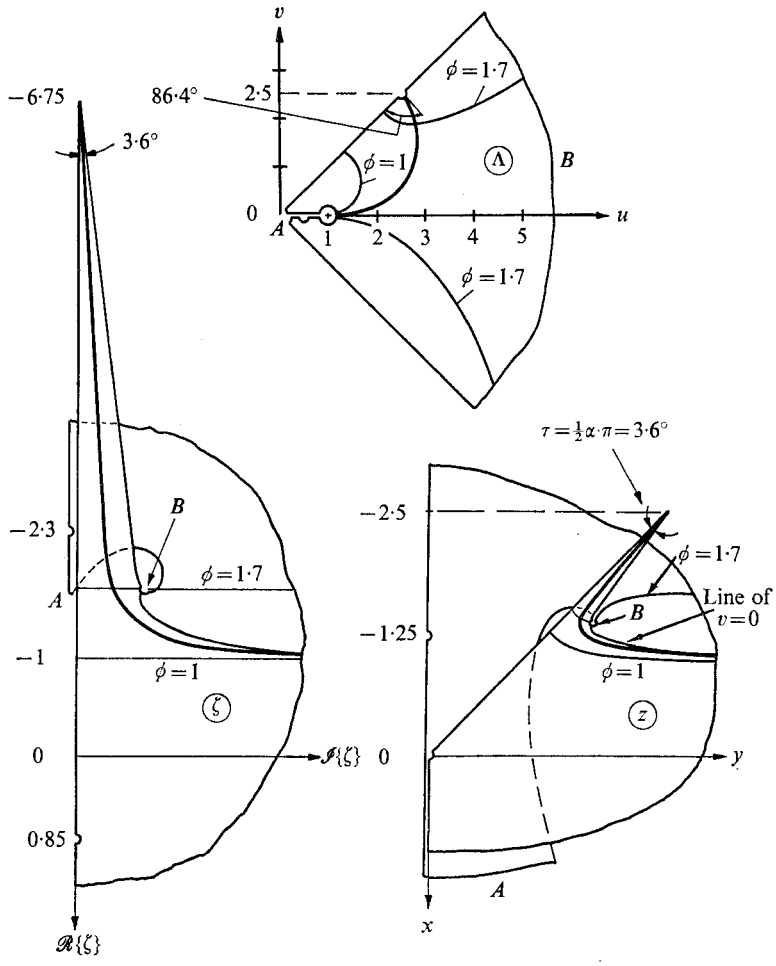

FIGURE 5. Hodograph uniform flow and wedge flow planes.

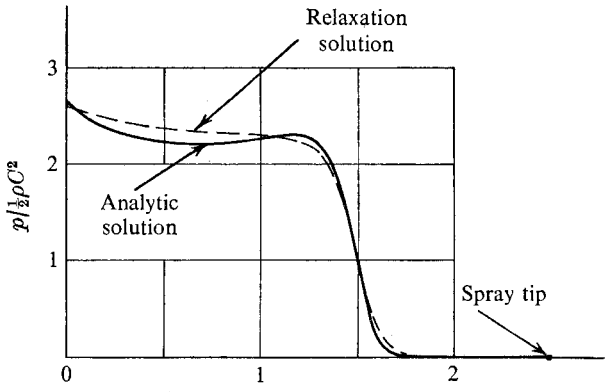

FIGURE 6. Wedge pressure distribution.

conditions are satisfied (which has been shown to be within 1 %), the error in the pressure distribution is considered to be of the same order of magnitude. The pressure obtained by the relaxation method of solution is also shown and is seen to be in good agreement with the present quasi-analytical solution.

Total force

The total hydrodynamic force F (per unit width) on the wedge is obtained by integrating the pressure over the projected area of the wedge face (both sides). This can be expressed in terms of a non-dimensional coefficient

$$C_F = \frac{F}{\rho C^2 D} = \int_1^{2\cdot5} \frac{p}{\frac{1}{2}\rho C^2} dy. \tag{10.2}$$

The above integral was evaluated from the pressure distribution of figure 6 and the coefficient C_F was found to be 3·40. The relaxation solution agreed closely with this, giving a value of 3·45. Dobrovolskaya (1969), on the other hand, obtained $C_F = 4{\cdot}10$.† This result differs appreciably from that of the present analysis, but since the above paper does not give any further details for the 90° case it is not possible to trace the source of this discrepancy. In any case, Dobrovolskaya's paper was mainly devoted to thin wedges and specifically states that the results presented for large wedge angles are only approximate.

A great deal of experimental work has also been conducted for the wedge problem. The U.S. National Bureau of Standards Report no. 6.4/1-196 (1949) shows that for wedges of intermediate nose angle (i.e. approximately 90°) the experimental values of C_F are best represented by Wagner's original expression

$$C_F = \pi \left(\frac{\pi}{2\sigma} - 1\right)^2, \tag{10.3}$$

in which σ represents the deadrise angle. For a 90° wedge $\sigma = \frac{1}{4}\pi$ and therefore the experimental value of C_F for this case is simply $C_F = \pi$. Thus, the present solution ($C_F = 3{\cdot}40$) for the ideal case differs from that of a real fluid by approximately 8 %. This discrepancy is almost certainly due to the effects of gravity and viscosity, both of which are ignored in the ideal case. For Dobrovolskaya's solution ($C_F = 4{\cdot}10$) the difference is approximately 30 %.

11. Experimental work; comparison of ideal and actual flows

In order to determine the extent to which the above solution for an ideal weightless fluid can be applied to the case of a real fluid in the presence of gravity, an experiment was conducted in which fluid velocities were measured in the entire near-field region of the flow. The experimental equipment consisted of a $6 \times 48 \times 48$ in. tank fitted with a clear plastic wall, a prismatic 6 in. wide 90° wedge mounted on a vertical guide shaft, a stroboscope and a camera. Small

† The actual value given in Dobrovolskaya (1969, figure 15) is 8·20 but the figure is in error because the factor of $\frac{1}{2}$ in the pressure coefficient was not taken into account in the calculation of C_F.

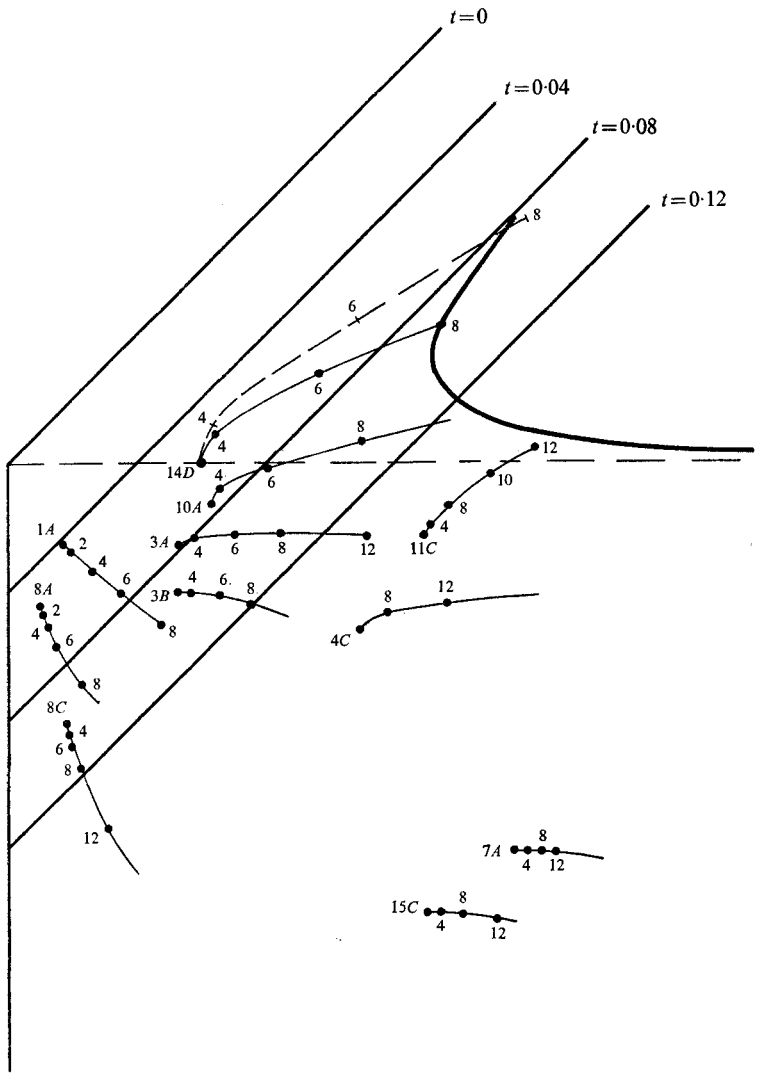

FIGURE 7. Sample particle paths. The figures 4, 6, 8, 10 and 12 labelling the prints refer to t = 0·04, 0·06, 0·08, 0·10 and 0·12 respectively.

(0·10 in. diameter) white polystyrene spheres of near-neutral density were used as marker particles and the high-speed flash of the stroboscope gave a multiple exposure. The density of the water was adjusted by the addition of salt in order to get a near-perfect match. The velocity of each particle was computed for each of its positions by means of finite-difference formulae. Since the particle paths are curved, this had to be done separately for the x and y directions. The wedge velocity was computed similarly and the particle velocities were then normalized by dividing by the wedge speed.

One of the important requirements is that the wedge speed be as nearly constant as possible. Preliminary testing revealed that variations of less than 3 % could be

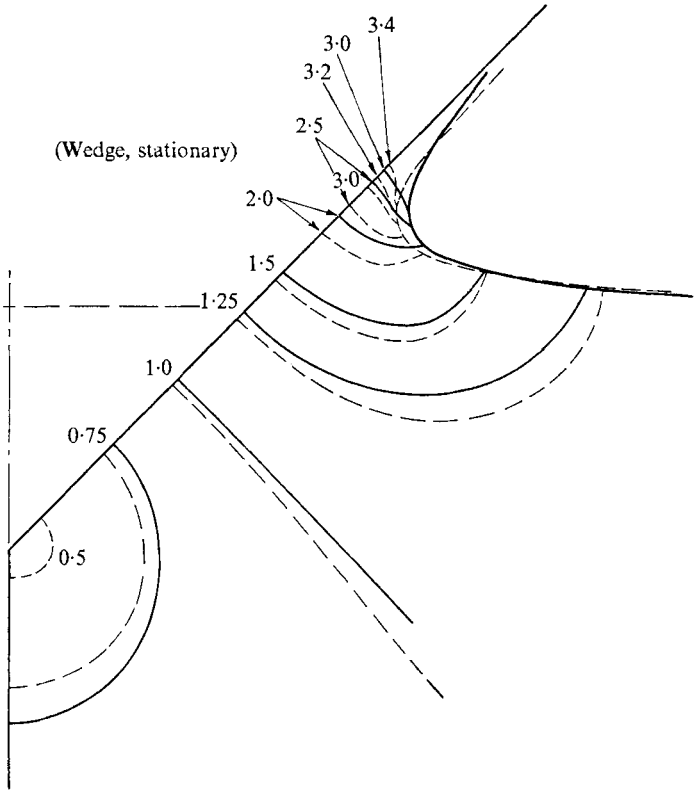

FIGURE 8. Total velocity: comparison of ideal (broken line) and experimental (solid line) results.

achieved for the first 5 in. of submergence by simply pushing the wedge manually. This was sufficient since, in order to guard against wall and bottom effects, it was intended to take readings only for this initial period of entry. Figure 7 shows some sample experimental results; the complete results are contained in Hughes (1971). Total velocity is shown in figure 8, in which, for purposes of comparison, the experimental flow has been converted to the case of a fluid moving past a stationary wedge. The contours of constant total velocity for the ideal case correspond to concentric circles in the Λ plane, centred about the origin. The curves agree closely over most of the fluid region but discrepancies are evident in the spray-root region and these become more pronounced in the spray jet. This is not surprising because the fluid in this region has passed along the entire face of the wedge and, since the jet is relatively thin, the resulting boundary layer would be expected to have a large effect. Also, since this region is very nearly a free jet, the downward pull of gravity will have its greatest effect here. This is evident in figure 8, in which the spray jet is much shorter and thicker than for the ideal flow, and this accounts for the disagreement in free-surface position.

Since the principle of similarity requires the absence of gravity, one of the objects of the experiment was to determine the extent to which gravity caused the actual flow to depart from this principle. This information can be readily

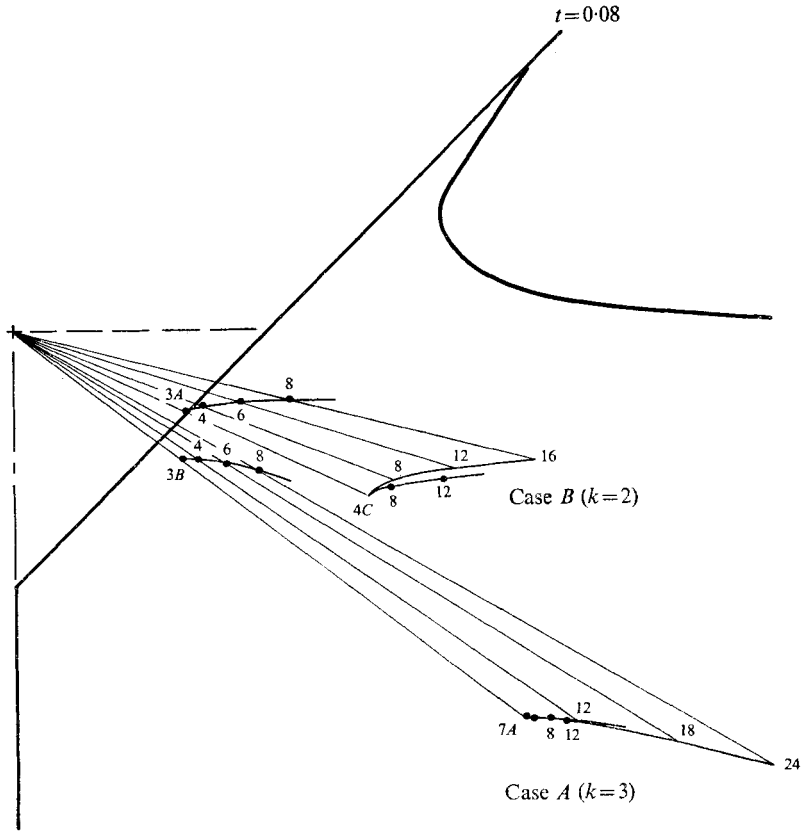

FIGURE 9. Geometric similarity: comparison of ideal and experimental results.

obtained from the experimental results since in several cases two different particles occupied positions which are geometrically similar. As an example, two such pairs of particles are shown in figure 9, in which the ratio of the initial radial distances of the outer and inner particle is denoted as k. The two pairs shown in figure 9 were selected because their distance ratio k is an integer, which means that every kth image of the outer particle corresponds to an image of the inner particle. Thus the extent to which similarity is attained is easily seen by multiplying each of the inner radii by k and comparing these positions with those of the corresponding outer particle. The resulting points in figure 9 show that the flow closely follows the principle of similarity over most of the flow field, with some departure near the free surface.

On the free surface itself, the particle path corresponding to geometric similarity can be computed for any particle on the basis of constant arc length from the spray tip. This is done in figure 7 for particle $14D$, and the divergence of the two paths shows clearly the extent to which gravity and viscosity prevent similarity from being achieved in the spray jet region.

We may also consider the effect which wedge velocity has in the above comparison. It can be shown from dimensional analysis that the acceleration of the fluid is proportional to the square of the wedge velocity. From this it is obvious that

for high-speed entry the relative effect of gravity will be small owing to the large fluid accelerations and the fluid will therefore follow a law of similarity more closely.

12. Concluding remarks

The computer method of conformal mapping presented above is quite general and can be applied to a wide variety of problems. The only requirement is that the transformation be localized in nature. If this is not the immediate situation, it can usually be achieved by using an approximate elementary mapping function for the gross transformation. This was the case in the above solution to the wedge entry problem, in which the elliptic-function transformation $T_e(W)$ was used for this purpose.

Also, the above solution can be further generalized to the case of a variable wedge speed. As was noted by Gurevich (1965), the principle of geometric similarity can be extended to cases in which the wedge speed is proportional to t^γ, where γ is an arbitrary constant. This would be a significant improvement since in most physical cases the penetrating body is slowing down owing to the action of the retarding force.

In conclusion, the hope is expressed that by providing information about the entire flow field, including such details as the spray-root and the spray-tip singularities, the above analysis of the wedge problem may be helpful in dealing with the more difficult problem of general free-surface penetration.

Appendix. Description of the preparatory transformation

This transformation was obtained by means of the computer-oriented method outlined in §6. The solution was achieved gradually, beginning with only one application of the basic mapping function $T_c(\Pi)$. Although very approximate, this solution indicated clearly that singularities occurred at, or near, the points $\Gamma = -\epsilon$ and $\Gamma = 0$ and these values were therefore assigned to κ_1 and λ_1 respectively. The solution was gradually improved by further applications of $T_c(\Pi)$. At each stage, the solution was examined to see what overall transformation was being generated and to search for cases in which the singularities in later mappings were located at the same points as those of earlier mappings. In such cases, the values of κ and λ could be computed from the earlier values. Also, in some other cases, the values of κ and λ were determined by problem requirements, such as symmetry.

The final result can best be described with the aid of figure 10, which shows that the solution consists of four applications of the basic mapping function $T_c(\Pi)$. Each involves three parameters, and another parameter Q was used in the third mapping, giving a total of thirteen. However, three of the parameter values (λ_3, λ_4 and κ_4) are determined from earlier values, as shown schematically in the upper left-hand corner of figure 10. Also, the singularities κ_1 and λ_1 of the first mapping are located at $-\epsilon$ and 0 respectively; the value of λ_2 is fixed from the symmetry of the second map ($\lambda_2 = -\kappa_2$) and the value of κ_3 is fixed by the requirement that the κ_2 point ($\Pi_2 = -Q + iK_2$) be transformed to the real axis

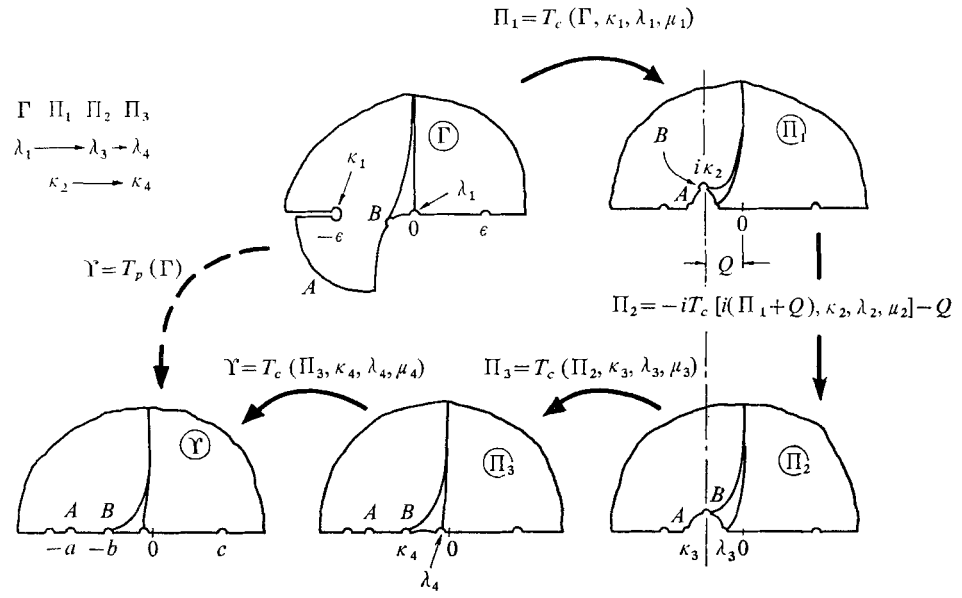

FIGURE 10. Preparatory transformation.

in Π_3. Thus a total of seven parameters can be calculated beforehand, leaving six undetermined parameters in the preparatory transformation ($\mu_1, \mu_2, \kappa_2, Q, \mu_3$ and μ_4). Further details of the solution may be obtained from the author.

REFERENCES

BISPLINGHOFF, R. L. & DOHERTY, C. S. 1952 Some studies of the impact of vee wedges on a water surface. *J. Franklin Inst.* **253**, 547.

BORG, S. F. 1957 Some contributions to the wedge-water entry problem. *J. Eng. Mech. Div., A.S.C.E.* **93**, Paper no. 1214.

DOBROVOLSKAYA, Z. N. 1963 Investigation of the motion of an incompressible fluid. *Appl. Math. Mech.* **27**, 1377.

DOBROVOLSKAYA, Z. N. 1964 *Sov. Phys. Dokl.* **8**, 1179.

DOBROVOLSKAYA, Z. N. 1969 *J. Fluid Mech.* **36**, 805.

FABULA, A. G. 1957 Ellipse-fitting approximation of impact of rigid bodies on water. *Proc. 5th Mid-western Conf. on Fluid Mech.* p. 299.

GARABEDIAN, P. R. 1953 Oblique water entry of a wedge. *Comm. Pure Appl. Math.* **6**, 157

GARABEDIAN, P. R. 1965 *Proc. Symp. on Appl. Math.* **17**.

GUREVICH, M. I. 1965 *Theory of Jets in Ideal Fluids*, p. 435. Academic.

HUGHES, O. F. 1971 Wedge penetration of a free surface. *School Mech. Indust. Eng., University of New South Wales Rep.* 1971/NA/2.

MAN, K. H. 1957 Studies of some problems about unsteady fluid motion. Ph.D. thesis, Moscow State University.

MILNE-THOMSON, L. M. 1938 *Theoretical Hydrodynamics*. Macmillan.

PIERSON, J. P. 1950 Penetration of a fluid surface by a wedge. *Stevens Inst. Tech. ETT Rep.* no. 381.

SHIFFMAN, M. & SPENCER, D. C. 1951 The force of impact on a cone striking a water surface. *Comm. Pure Appl. Math.* **4**, 379.

WAGNER, H. 1932 Über Stoss Gleitvorgange an der Oberflache von Flussigkeiten. *Z. angrew. Math. Mech.* **12**, 193.